Neuroscience 256 (2014) 456–466

INTRACELLULAR NOGO-A FACILITATES INITIATION OF NEURITE FORMATION IN MOUSE MIDBRAIN NEURONS *IN VITRO*

Z. KUROWSKA,[a,b*] P. BRUNDIN,[c,d] M. E. SCHWAB[e] AND J.-Y. LI[a]

[a] *Neural Plasticity and Repair Unit, Wallenberg Neuroscience Center, Lund University, BMC A10, 22184 Lund, Sweden*

[b] *Neurodegeneration and Inflammation Genetics Unit, Wallenberg Neuroscience Center, Lund University, BMC A10, 22184 Lund, Sweden*

[c] *Neuronal Survival Unit, Wallenberg Neuroscience Center, Lund University, BMC B11, 221-84 Lund, Sweden*

[d] *Van Andel Research Institute, Center for Neurodegenerative Science, 333 Bostwick Avenue NE, Grand Rapids, MI 49503, USA*

[e] *Brain Research Institute, University of Zürich, Department of Health Sciences and Technology, ETH Zürich, 190 Winterthurerstrasse, 8057 Zürich, Switzerland*

Abstract—Nogo-A is a transmembrane protein originally discovered in myelin, produced by postnatal CNS oligodendrocytes. Nogo-A induces growth cone collapse and inhibition of axonal growth in the injured adult CNS. In the intact CNS, Nogo-A functions as a negative regulator of growth and plasticity. Nogo-A is also expressed by certain neurons. Neuronal Nogo-A depresses long-term potentiation in the hippocampus and modulates neurite adhesion and fasciculation during development in mice. Here we show that Nogo-A is present in neurons derived from human midbrain (Lund human mesencephalic (LUHMES) cell line), as well as in embryonic and postnatal mouse midbrain (dopaminergic) neurons. In LUHMES cells, Nogo-A was upregulated threefold upon differentiation and neurite extension. Nogo-A was localized intracellularly in differentiated LUHMES cells. Cultured midbrain (dopaminergic) neurons from Nogo-A knock-out mice exhibited decreased numbers of neurites and branches when compared with neurons from wild-type (WT) mice. However, this phenotype was not observed when the cultures from WT mice were treated with an antibody neutralizing plasma membrane Nogo-A. *In vivo*, neither the regeneration of nigrostriatal tyrosine hydroxylase fibers, nor the survival of nigral dopaminergic neurons after partial 6-hydroxydopamine lesions was affected by Nogo-A deletion. These results indicate that during maturation of cultured midbrain (dopaminergic) neurons, intracellular Nogo-A supports neurite growth initiation and branch formation.

Key words: Nogo-A, Parkinson's disease, midbrain dopaminergic neurons, neurite growth, cell culture.

INTRODUCTION

Nogo-A is a transmembrane protein originally discovered in the adult CNS. Nogo-A belongs to the reticulon family – ubiquitous transmembrane proteins enriched in the endoplasmic reticulum. At present, the biological functions of the majority of reticulons are unknown (Schwab, 2010). Nogo-A, in contrast to the shorter isoforms Nogo-B and -C or other reticulons, is highly enriched in the CNS. In the adult CNS Nogo-A is primarily expressed by oligodendrocytes and myelin and by subpopulations of neurons (Caroni and Schwab, 1988; Huber et al., 2002; Wang et al., 2002). The neurite growth inhibitory effects of Nogo-A are mediated by a receptor complex, which includes NgR-1, p75/TROY and Lingo1 as well as additional, yet uncharacterized components. The receptor(s) activate(s) the RhoA/ROCK pathway (Fournier et al., 2003; Yiu and He, 2006; Montani et al., 2009), resulting in growth cone collapse and inhibition of axonal growth in injured, but also in intact adult CNS (Schwab, 2010).

In addition, Nogo-A is also expressed by subpopulations of neurons, particularly during development (Huber et al., 2002; Mathis et al., 2010; Petrinovic et al., 2010, 2013). Migration of some types of neurons is restricted by Nogo-A expression (Mingorance-Le Meur et al., 2007; Mathis et al., 2010). Nogo-A function blocking during development causes aberrant growth of the peripheral neurites *in vitro* and nerves *in vivo* (Petrinovic et al., 2010). Later in development, Nogo-A affects the plasticity of the visual cortex and other parts of CNS (Kapfhammer and Schwab, 1994; McGee et al., 2005). Nogo-A/NgR-1 signaling also negatively regulates long-term potentiation (LTP) at hippocampal synapses (Raiker et al., 2010; Delekate et al., 2011; Tews et al., 2013) as well as axonal and dendritic sprouting and plasticity (Zagrebelsky et al., 2010; Petrinovic et al., 2013).

Dopaminergic neurons located in the ventral midbrain are critical for cognitive and motor behavior and are

*Correspondence to: Z. Kurowska, Neurodegeneration and Inflammation Genetics Unit, Wallenberg Neuroscience Center, Lund University, BMC A10, 22184 Lund, Sweden. Tel: +46-46-2220635; fax: +46-46-2220531.

E-mail address: zuzanna.kurowska@med.lu.se (Z. Kurowska).

Abbreviations: 6-OHDA, 6-hydroxydopamine; ANOVA, analysis of variance; DAB, 3,3′-diaminobenzidine; DAPI, 4′,6-diamidino-2-phenylindole; DMEM, Dulbecco's Modified Eagle Medium; EDTA, ethylenediaminetetraacetic acid; FCS, fetal calf serum; GDNF, Glial cell line-derived neurotrophic factor; HBSS, Hanks Balanced Salt Solution; HRP, horseradish peroxidase; KO, knock-out; LUHMES cells, Lund human nesencephalic cells; PBS, phosphate-buffered saline; PBST, PBS with 0.3% Triton X-100; PFA, paraformaldehyde; RCF, relative centrifugal force; SDS–PAGE, sodium dodecyl sulfate polyacrylamide gel electrophoresis; TH, tyrosine hydroxylase; WT, wild-type.

0306-4522/13 $36.00
http://dx.doi.org/10.1016/j.neuroscience.2013.10.029

associated with multiple CNS disorders. Substantia nigra (A9) neurons have been extensively studied, as the slow degeneration of the nigrostriatal pathway is responsible for the motor defects observed in Parkinson's disease patients (Hornykiewicz, 1966; Riederer and Wuketich, 1976). While Parkinson's disease is linked to specific genetic mutations only in the minority of cases (5–10% of all Parkinson's disease patients), about 40% of sporadic cases are attributed to unknown genetic risk factors (Hamza et al., 2010). Some studies showed evidence for polymorphisms and differential expression of genes involved in axonal growth in patients with Parkinson's disease (Lesnick et al., 2007; Bossers et al., 2009). We were therefore encouraged to investigate the roles of Nogo-A in developing and adult intact midbrain dopaminergic neurons and in the parkinsonian mouse model. Such an investigation, which could potentially lead to better understanding of Parkinson's disease pathogenesis, has not been, to our knowledge, reported before.

In our study we have first assessed, whether Nogo-A is present in the prenatal and postnatal nigral dopaminergic neurons. Second, we studied wild-type (WT) and Nogo-A knock-out (KO) mice and employed *in vitro* and *in vivo* models to establish whether constitutive deletion, or neutralization of the Nogo-A on the plasma membrane has an impact on survival and neurite outgrowth in midbrain dopaminergic neurons.

EXPERIMENTAL PROCEDURES

Lund human mesencephalic (LUHMES) and MN9D cell cultures

The Lund human mesencephalic (LUHMES) cell line was kindly provided by Dr. Marcel Leist (Konstanz, Germany). Originally, the LUHMES cell line was obtained from a subclone of MesC2.10, a conditionally immortalized, non-transformed cell line derived from human ventral mesencephalon embryonic tissue (Lotharius et al., 2002). LUHMES cell maintenance and differentiation were performed as previously described (Scholz et al., 2011). Briefly, for LUHMES maintenance and differentiation plastic 6-well plates (Nunc, Penfield, NY, USA) or glass Nunc Lab-Tek chambered coverglass slides (Thermo Scientific, Waltham, MA, USA) pre-coated with 50 μg/mL poly-L-ornithine and 1 μg/mL fibronectin (Sigma–Aldrich, St. Louis, MO, USA) were used. Proliferation medium consisted of Advanced Dulbecco's modified Eagle's medium/F12 (Gibco, Carlsbad, CA, USA), N-2 supplement (Invitrogen, Carlsbad, CA, USA), 2 mM L-glutamine (Sigma–Aldrich) and 40 ng/mL recombinant basic fibroblast growth factor (bFGF, R&D Systems). For differentiation, medium consisting of Advanced Dulbecco's modified Eagle's medium/F12, N-2 supplement, 2 mM L-glutamine, 1 mM dibutyryl cAMP (Sigma–Aldrich), 1 μg/mL tetracycline (Sigma–Aldrich) and 2 ng/mL recombinant human Glial cell line-derived neurotrophic factor (GDNF, R&D Systems, Minneapolis, MN, USA) was used. For enzymatic detachment and dissociation LUHMES cells were incubated with antibiotic-trypsin-Versene (ATV) trypsin (138 mM NaCl, 5.4 mM KCl, 6.9 mM $NaHCO_3$, 5.6 mM D-Glucose, 0.54 mM EDTA, 0.5 g/L trypsin from bovine pancreas type-II-S; Sigma–Aldrich) for 3 min in 37 °C and then spun down in 300 relative centrifugal force (RCF) for 5 min. Differentiation of LUHMES cells had two steps: 24 h after plating, the differentiation was initiated by changing from proliferation to differentiation media. After additional 48 h we enzymatically detached and re-plated the cells to new dishes for 3 additional days of differentiation (medium was changed 48 h after re-plating). We plated 1.5×10^5 cells/cm^2 for imaging and 2.5×10^5 cells/cm^2 for protein harvest in the re-plating step. Undifferentiated LUHMES we seeded with density of 2.0×10^4 cells/cm^2 and proteins were harvested 2 days after.

The MN9D cell line was kindly provided by Dr. A. Heller (University of Chicago, Chicago, IL, USA). Originally, the MN9D cell line was obtained by hybridoma fusion of cells from murine mesencephalic cells with neuroblastoma cells (Choi et al., 1991). MN9D cells, when differentiated have properties of midbrain dopaminergic neurons, i.e. they express dopaminergic markers and release dopamine (Choi et al., 1991, 1992; Rick et al., 2006). The cells were maintained as previously described (Choi et al., 1991). Briefly, the cells were grown in Dulbecco's Modified Eagle Medium/F12 (DMEM/F12) medium with L-glutamine (Gibco), supplemented in 10% fetal calf serum (FCS, Gibco) and penicilin/streptomycin (100 U/mL/100 mg/mL, Gibco). For differentiation, the cells were seeded in density of 3×10^3 cells/cm^2 and after 24 h sodium butyrate (1 mM) was added and the cells were cultured for the next 7 days.

In our experiments, we used undifferentiated (day 0) and differentiated LUHMES and MN9D cells. The differentiation state in both cases was verified by immunocytochemical labeling of tyrosine hydroxylase (TH), the key enzyme for dopamine synthesis, and the morphology (neurite growth and neurite network formation). LUHMES cells were considered 'differentiated' after 5 days of differentiation (Scholz et al., 2011), and MN9D cells, after 7 days (Rick et al., 2006).

Nogo-A Western-blot analysis

We performed eight independent protein extractions from undifferentiated ($n = 4$) and differentiated ($n = 4$) LUHMES cells and extractions in duplicate for undifferentiated and differentiated MN9D cells. Cells were lysed in buffer composed of: 20 mM Tris (pH 7.4), 150 mM NaCl, 5 mM EDTA, 0.5% NP-40 and protease inhibitor cocktail (1:100, P8849, Sigma–Aldrich). Protein concentration was measured using Bradford reagent (Sigma). Following boiling in Laemli buffer, eight micrograms of total proteins ware loaded onto 8% sodium dodecyl sulfate polyacrylamide gel electrophoresis (SDS–PAGE) gel. After the transfer onto Immuno-Blot® polyvinylidene difluoride (PVDF) membranes (Bio-Rad, Hercules, CA, USA), proteins were blocked with 5% milk in 0.05% phosphate-buffered saline (PBS)–Tween-20 for 2 h at room temperature. Next, the membrane was incubated with the primary antibody over-night at 4 °C, in 3% milk and PBS–

Tween-20. Following washing steps, horseradish peroxidase (HRP)-conjugated secondary antibody was applied onto the membrane for 1 h at room temperature. For visualization, we used the ECL Western blotting luminol reagent (sc-2048, Santa Cruz Biotechnology, Inc., Sweden). We used primary antibodies against Nogo-A (11C7, 1:5000) or GAPDH (1:5000, ab9485, Abcam, UK) and secondary HRP-conjugated antibodies: anti-mouse HRP and anti-rabbit (P0447 and P0448, respectively 1:10,000, Dako, Sweden).

11C7 is a monoclonal antibody raised against rat/mouse Nogo-A peptide sequence 623–640 (Oertle et al., 2003). This antibody does not bind to Nogo-B and -C (Oertle et al., 2003; Dodd et al., 2005). 11C7 has been used previously to detect Nogo-A in mouse and human samples, both in Western-blot and in immunohistochemical stainings (Bandtlow et al., 2004; Buss et al., 2005; Montani et al., 2009; Lackner et al., 2011). Although Nogo-A has an estimated molecular weight of 139 kDa, it migrates as a protein of 220 kDa on SDS–PAGE gel (Chen et al., 2000; Dodd et al., 2005). For densitometric measurements of luminescent signal in LUHMES cell extracts, the ImageJ 1.42q software (Version 1.42q; National Institutes of Health, USA) was used. The densitometric measurements of Nogo-A and GAPDH (39 kDa) bands were diminished by the value of background and then the averaged value from 'differentiated' samples was normalized to average value of 'undifferentiated' samples.

Ethics statement

In all procedures conducted in this study special care was taken to minimize the number and suffering of experimental animals. All procedures in this study that involved mice were approved by the Ethics Committee for the use of laboratory animals at the Lund University (Permit No.: M76-09).

Nogo-A KO and WT mice

We used Nogo-A^{-}/$^{-}$ (KO) mice in 129X1/SvJ background (Dimou et al., 2006) and 129X1/SvJ 000961 WT controls (The Jackson Laboratory, USA). Nogo-A KO mice lack Nogo-A protein expression, but do express the –B and –C isoforms of Nogo. The detailed description of the construct has been published previously (Simonen et al., 2003; Dimou et al., 2006). The animals were housed under standard conditions with free access to food and water under a standard 12-h light–dark regime (light 07.00–19.00 h). Experimental groups were composed of balanced numbers of male and female adult mice (12–13 weeks old).

Mouse embryonic tissue preparation

The morning of plug detection in WT or Nogo-A KO mice was considered as the embryonic day 0.5 (E0.5). At the E13.5 the pregnant mice were killed by cervical dislocation and the embryos were immediately isolated and their heads were post-fixed (4% paraformaldehyde, PFA) for 6 h at 4 °C, and then transferred to 30% sucrose in PB at 4 °C for cryoprotection over night. The whole embryos were immersed in O.C.T. (BDH Prolabo, VWR, Leuven, Belgium) and the heads were cut on cryostat in 15-μm coronal sections. The sections were collected on Super Frost Ultra Plus® slides (Thermo Scientific, USA) and dried over night at 4 °C, then immuno-stained.

Ventral mesencephalon primary culture preparation

The procedure of mesencephalon primary culture preparation was performed as previously described (Pruszak et al., 2009), with slight modifications. The procedure was performed aseptically in a timely manner and the embryos or the embryonic tissues were always kept on ice in sterile Hanks Balanced Salt Solution (HBSS) without Ca^{2+} and Mg^{2+} (Sigma). At E13.5 the pregnant WT or Nogo-A KO mice were killed and the embryos were immediately aseptically isolated from the uterine horns.

After removing the uterine sac and amniotic membranes, embryos were moved to fresh HBSS solution and decapitated. The skull layer was removed from the brain and the rostral forebrain and caudal hindbrain regions were removed resulting in a remaining tube-like structure of the midbrain. Cutting the mesencephalon tube along the dorsal midline, the flat butterfly-structure was obtained, which was then trimmed along the dorsal edges to remove 2/3 of dorsal tissue. Following the additional mechanical dissociation of ventral midbrain tissue pieces into small chunks (< 1 mm), trypsin was applied to obtain a single cell suspension: 0.1% Trypsin (Gibco), 0.05% DNAze (Sigma-Aldrich), 20 min, 37 °C. Tissues were then additionally dissociated by gentle pipetting and centrifuged (300 RCF, 5 min, 4 °C), and finally dissolved in DMEM medium (Gibco) containing 5% of FCS (Gibco). 7.0×10^4 cells per cm^2 were plated on coated glass slides (0.01% poly-L-lysine and 5 μg/mL fibronectin, Sigma) in 24-well plates and after 24 h the initial medium was replaced by serum-free medium: DMEM/F12 with Glutamax (Gibco), B27, 10 ng/mL of human recombinant GDNF (R&D Systems). Serum-free medium was changed every other day and after 6 days the cells were fixed (with 4% PFA, 20 min in room temperature) and after a brief washing with PBS, kept in the fridge until staining was performed. In order to block receptor-mediated action of Nogo-A in cultures with WT cells, the antibody 11C7 was added (10 μg/mL) together with each serum-free medium change. 11C7 was raised against an 18-amino acid Nogo-A peptide corresponding to the mouse/rat sequence of amino acids 623–640 (Oertle et al., 2003) and similar concentrations were previously used to neutralize delta-20/Nogo-A receptor signaling in neuronal *in vitro* mono-cultures (Dodd et al., 2005; Montani et al., 2009; Petrinovic et al., 2010). In those systems, neurite growth and growth cone motility changes were observed upon administration of 11C7 vs. controls. Twelve independent ventral mesencephalon primary culture experiments – WT ($n = 4$), WT with 11C7 ($n = 4$) and Nogo-A KO mice ($n = 4$) – were performed. Typically, in each experiment tissues from

5–7 embryos from one pregnant mouse were combined and the cells were plated in four wells. After 7 days *in vitro* the percentage of differentiated TH-positive neurons in WT, 11C7-treated WT and Nogo-A KO cultures was similar, on average 8.4 ± 8.7, 13.3 ± 5.5 and 1.3 ± 2.5 (± S.D.), respectively.

6-Hydroxydopamine (6-OHDA) injections

6-OHDA (Sigma, Sweden) was injected into the right striatum under isoflurane anesthesia and analgesia (1.5–2% isoflurane in 1:2 of oxygen:nitrous oxide), using a stereotaxic mouse frame (Stoelting, Germany) and a 5 μL Hamilton syringe fitted with a fine glass capillary. The toxin was used at a concentration of 8 μg/μL, dissolved in a solution of 0.02% ascorbic acid in 0.9% sterile saline. A total volume of 1 μL was injected using the stereotaxic coordinates: A/P = + 0.5 mm, M/L = –2.0 mm, D/V = –3.0 mm, with a flat skull position and all coordinates measured from bregma. Injections were made at a rate of 0.25 μL/15 s. We maintained the capillary in place for an additional 3 min to allow the toxin to diffuse. After removing the needle, the wound was cleaned and sutured and the mouse was injected with 75 μg of bupivacaine around the wound, to diminish pain. We administered the 6-OHDA being blinded for the genotype. In the first group of animals that we investigated (4 weeks time point), three out of eight mice in Nogo-A KO group died unexpectedly 1, 4 and 7 days following the lesion. In following experiments, we took special care of animals (glucose injections 50 mg/mL and feeding with food extruded in 30% sucrose), successfully avoiding these unexpected dropouts in two other groups ('4 days' and '8 weeks').

Adult mouse tissue preparation

Mice were sacrificed 4 days, 4 weeks or 8 weeks after the 6-OHDA lesions. Animals were anaesthetized with an overdose of sodium pentobarbitone i.p. (Apoteket AB, Solna, Sweden) and then were transcardially perfused with 15 mL of room-temperature 0.9% saline, followed by 100 mL of ice-cold 4% PFA in 0.1 M PBS. Brains were post-fixed over night at 4 °C and then transferred to 30% sucrose in PB at 4 °C for cryoprotection overnight. The brains were then sectioned in the coronal plane using a microtome at a thickness of 40 μm. Sections were collected in six series and stored at 4 °C in 0.01% sodium azide in PBS until free-floating immunohistochemistry was performed.

Immunohistochemical fluorescent staining

For staining of Nogo-A in LUHMES cells, cells were fixed with 4% PFA for 20 min at room temperature and then the following steps were performed: triple rinse with PBST (PBS with 0.3% Triton X-100), 1 h blocking with 5% normal donkey serum in PBST at room temperature, incubation with primary antibodies – anti-Nogo-A (sc-25660, 1:200, Santa Cruz Biotechnology, Dallas, TX, USA) and anti-beta III-tubulin (1:200, T2200, Sigma) – in PBST over night at 4 °C, triple rinse with PBST, incubation with secondary antibodies DyLight488 (715-485-151) and Cy3 (711-165-152, Jackson Immuno-Research Inc., West Grove, PA, USA) in PBST for 2 h at room temperature, 10-min incubation with 4′,6-diamidino-2-phenylindole (DAPI), (1:1000, Sigma) in PBST, triple PBST rinse, covering with a layer of DABCO medium (Sigma–Aldrich). In case of plasma membrane Nogo-A staining in LUHMES cells, we washed the cells in PBS and placed on ice. Then the cells were washed with cold HBSS containing 1 mM $CaCl_2$ and 0.5 mM $MgCl_2$ and blocked with cold 10% serum for 20 min on ice, and following, the anti-Nogo-A antibody sc-25660 (1:50, Santa Cruz Biotechnology) or anti-Ret sc-13104 (1:50, Santa Cruz Biotechnology) antibody in blocking solution was added to the cells for 30 min. The cells were then transferred to room temperature and fixed with 4% PFA for 20 min and the secondary antibodies were applied as described above. In case of staining of mouse tissues, both embryonic and adult, the unspecific binding of monoclonal primary antibodies with mouse antigens was avoided by the application of 'Mouse on Mouse' solution (M.O.M.BMK-2202, Vector Laboratories Inc., Burlingame, CA, USA) before the blocking step. We used the primary antibodies anti-Nogo-A monoclonal 11C7 (1:1000) or polyclonal sc-25660 (1:200, Santa Cruz Biotechnology) together with anti-TH polyclonal P40101-0 (1:500, Pel-Freez, Rogers, AR, USA) or monoclonal 22941 (1:1000, ImmunoStar Inc., Hudson, WI, USA) for the adult and embryonic tissues, respectively, and followed the protocol described above. In the immunocytochemical staining of primary cultures derived from mouse embryonic ventral mesencephalon we used primary antibodies anti-TH and anti-beta-III tubulin (1:1000, TuJ1, Covance, Princeton, NJ, USA) and followed the staining protocol described above.

Immunohistochemical 3,3′-diaminobenzidine or diaminobenzidine (DAB) staining

Sections were rinsed in PBS and then endogenous peroxidase activity was quenched in 3% H_2O_2 and 10% methanol in PBS for 20 min. After rinsing steps, the sections were incubated in a blocking solution consisting of 5% normal goat serum in PBST and 0.3% Triton X-100 for 1 h, to block nonspecific binding sites. Sections were then incubated overnight at room temperature in the same blocking solution as described above with the primary antibody, rabbit anti-TH (1:1000, P40101-0, Pel-Freez). Then the sections were incubated in blocking solution for 20 min before 1 h incubation in a 1:200 dilution of biotinylated secondary antibody (Vector Laboratories, UK), in blocking solution. The sections were then treated with avidin–biotin–peroxidase complex (ABC Elite kit; Vector Laboratories, UK) in PBS for 1 h. The color reaction was developed by incubation in DAB (Vector Laboratories) for 1 min. Sections were mounted on gelatin-coated glass slides, dehydrated in an ascending series of alcohols, cleared in xylene and cover-slipped with DPX mounting medium (BDH Chemicals, VWR, Dawsonville GA 30534, USA).

Imaging

For the confocal imaging of immunolabeled LUHMES cells and mouse sections the LSM510 microscope was employed (Zeiss). The dimensions of images, the objective and zoom factor are indicated in figure legends.

We used Eclipse 80*i* microscope (Nikon, Tokyo, Japan) to obtain bright field images of DAB staining (objectives 1× and 4×) and images of fluorescently labeled primary culture (10×). Randomly sampled images of triple-labeled ventral midbrain neurons *in vitro* were obtained (7–9 per well) and then analyzed by the Cellomics software.

Cellomics analysis

We employed vHigh Content Screening (Thermo Fisher Scientific, Cellomics, Pittsburgh, PA, USA) software to perform optimization and analysis of the neurite growth in ventral mesencephalon cells obtained from Nogo-A KO, WT untreated and 11C7 treated embryos. Our protocol was optimized based on the Neuronal-Profiling.V4 algorithm, assay version 6.0.0.4008. Using the software, we first localized single particles (cell nuclei) based on circularity, size and total and average intensity of DAPI staining, and defined the exclusion criteria. Next, the thresholds were adjusted so that the program recognizes the majority of the beta-III tubulin-stained cell bodies, together with their processes as valid (e.g. one nucleus per cell body), despite minor differences in staining derived from some variety in each experimental repeat. To identify and validate the beta-III tubulin and TH-stained neurites, we have configurated the assay parameters by adjusting the following thresholds: for beta-III tubulin staining – cell body nucleus count, cell body total/average intensity, neurite length (25–400 μm); for TH staining – total/average intensity. The software identified the 'neurite points' (branching or crossing neurites) and excluded the cross points, leaving the validated branch points. All settings, although set initially by the Cellomics software, were optimized by the user via visible inspections of all images. There were up to 1772 cells sampled per experiment, and on average around 400 beta-III tubulin-positive neurons recognized per well (in the WT, WT with 11C7 and Nogo-A KO cultures, respectively).

Densitometry

We captured images from the TH-immunostained sections using (Eclipse 80*i*) microscope (Nikon). In all brains, we measured the extent of striatal denervation, as a consequence of lesion, by densitometry in dorsal and ventral striatum from 5–6 sections, corresponding to +1.2 mm to −1.0 mm from bregma. Using ImageJ 1.42q software (Version 1.42q; National Institutes of Health, USA), we measured intensity values. After subtracting the values of nonspecific background in the corpus callosum, values from all sections were averaged to provide a single value per animal. Optical intensity was normalized to the optical intensity value from the corresponding area of the intact hemisphere.

Cell counting in substantia nigra

We counted TH-positive neurons in substantia nigra pars compacta in ipsi- and contralateral site of the lesion using a stereological microscope. The borders defining the substantia nigra and ventral tegmental area on all levels along the rostrocaudal axis were defined using a low-power objective lens (4×). The medial border of the substantia nigra and lateral border of the ventral tegmental area were defined by a vertical line passing through the medial tip of the cerebral peduncle (and by the medial terminal nucleus of the accessory optic tract, when present in sections). The ventral border followed the dorsal border of the cerebral peduncle, thereby excluding the TH-positive cells in the pars reticulata, and the area extended laterally to include the pars lateralis in addition to pars compacta. This typically yielded up to 3–4 sections in a 1:6 series. The counting was done using a 40× objective on a Olympus BX50 microscope Olympus BX50 microscope equipped with a Marzhauser X–Y–Z step motor stage and the Visiopharm Integrator System software, Visiopharm A/S. All three axes and the input from the digital camera were controlled using the software that utilized a random start systematic sampling routine. During the whole procedure we were blinded for genotype. All the TH-positive cells seen in left and right nigra were counted. Cell survival values were obtained expressing averaged number of cells from ipsilateral as a proportion of averaged number of cells in contralateral side of an animal. The average number of TH-positive neurons counted in the intact substantia nigra was very similar in the WT and Nogo-A KO mice, 163.7 ± 50.9 and 172 ± 41.8 (± S.D.), respectively.

Statistics

All statistical analyses we conducted using Microsoft® Excel® for Mac 2011 Version 14.1.4 (Student *t*-test) or Prism 5.0c 2009, GraphPad Software, USA (for analysis of variance (ANOVA) and post hoc tests). Student *t*-test (2-tailed, 2 degrees of freedom) we employed for Western-blot data analysis. We used one-way ANOVA with Tukey post hoc test and two-way ANOVA with Bonferroni's multiple comparison to examine the nerite properties in vitro and DAB staining results, respectively.

RESULTS

Nogo-A is expressed in ventral mesencephalon-derived dopaminergic cell lines

First, we have employed a human dopaminergic neuronal cell line derived from embryonic mesencephalon (LUHMES cells) (Lotharius et al., 2005) to investigate Nogo-A expression. The LUHMES cells express neuroblast and stem cell markers and bare neuronal characteristics. Upon differentiation, LUHMES cells develop an extensive neurite network, reveal spontaneous electrical activity and express synaptic markers (Scholz et al., 2011), as well as several genes involved in dopamine uptake and release (Schildknecht et al., 2009; Scholz et al., 2011).

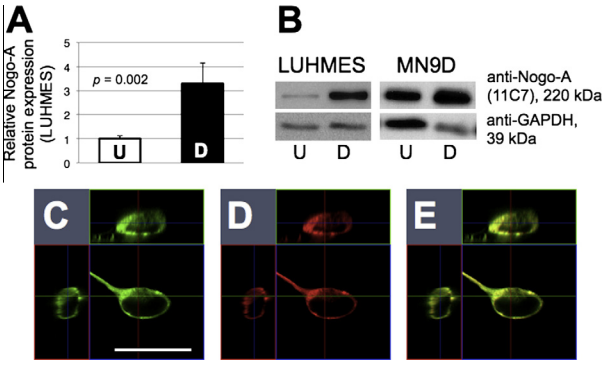

Fig. 1. Nogo-A is expressed by differentiated mesencephalic dopaminergic neurons *in vitro*. Using Western-blot, Nogo-A (220 kDa) was identified in the protein extracts from human mesencephalon-derived (LUHMES) cell line, in undifferentiated (U) and differentiated state (D), (n = 4, 2-tailed t-test) (A). The representative Western-blot results for LUHMES as well as equivalent mouse MN9D cell line before and after differentiation were depicted (B). The 3-D reconstructed confocal microscopic images (C–E) shown intracellular presence of Nogo-A (green) overlapping with beta-III tubulin staining (red), in the differentiated fixed permeabilized LUHMES cells (C – Nogo-A, D – beta-III tubulin, E – merged C, D). Plan Apochromat 40×/1.3, zoom 5x/6x (C–E). Scale bar = 20 μm. (For interpretation of the references to color in this figure legend, the reader is referred to the web version of this article.)

We have found that Nogo-A protein was present in the whole cell lysates of LUHMES cells before and after differentiation (Fig. 1), but the expression level was three times higher in differentiated than in the undifferentiated LUHMES cells (Fig. 1A, B). A similar expression pattern was observed in undifferentiated and differentiated mouse neuronal dopaminergic cell line, MN9D (Fig. 1B). We found that high levels of Nogo-A were present in the cytoplasm of vast majority of differentiated LUHMES cells (Fig. 1C–E). No intracellular labeling was observed when the same staining protocol was applied to a microglial cell line (BV2) *in vitro* as a negative control (data not shown). The staining on the non-fixed non-permeabilized LUHMES cells revealed plasma membrane localization of Nogo-A in only few cells in the differentiated state (data not shown).

These results show that Nogo-A protein is present in human- and mouse-derived dopaminergic neuronal cell lines and it is upregulated upon maturation *in vitro.* In most of the human midbrain-derived dopaminergic neurons studied *in vitro,* Nogo-A has intracellular localization.

Nogo-A is expressed by dopaminergic neurons in the mouse embryo and in adult mouse substantia nigra

TH is the rate-limiting enzyme of dopamine synthesis and it is well established as a marker of dopaminergic neurons. TH expression in the mouse midbrain begins prenatally at E11-12 (Zhou et al., 1995; Maxwell et al., 2005) and it is maintained throughout lifetime (Ivanova and Beyer, 2003). In the adult, TH expression progressively declines in substantia nigra pars compacta (Emborg et al., 1998; Chu et al., 2002).

By performing immunohistochemical double-labeling for TH together with Nogo-A in WT and Nogo-A KO mice, we were able to show the expression of Nogo-A in dopaminergic neurons of mouse embryonic midbrain (Fig. 2) and also confirm its presence in the dopaminergic neurons of adult mice midbrain (Fig. 3) (Wang et al., 2002). In the ventral mesencephalon (Fig. 2) of an E13.5 mouse embryo, Nogo-A labeling was present in the cytoplasm of many of the TH-positive neurons (Fig. 2B–D) but also in some cells surrounding the midbrain region. In contrast, the same double labeling performed on midbrain sections of Nogo-A KO embryos gave only low background fluorescent signals. The majority of neurons of the E15.5 mouse cortex were also positive for Nogo-A with slightly higher intensity than in the midbrain neurons (data not shown). Similar staining patterns as in the embryonic midbrain were observed in the corresponding dopamine neurons in the adult brain: the substantia nigra pars compacta (Fig. 3), which derives from part of the embryonic

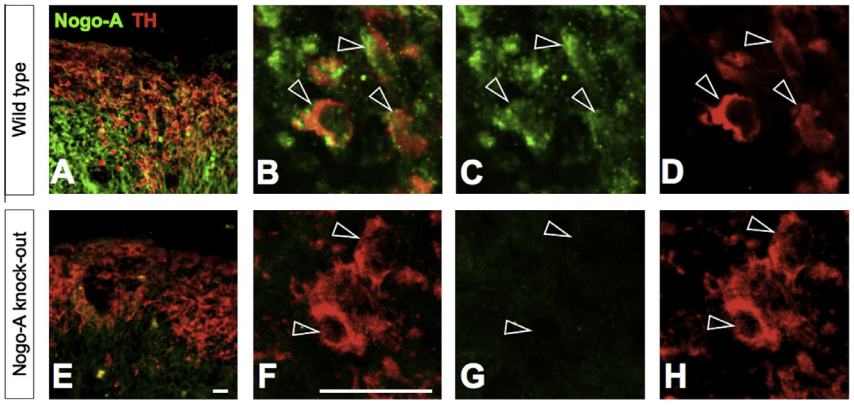

Fig. 2. Nogo-A is expressed in mouse embryonic ventral mesencephalon neurons. Confocal images show double labeling of Nogo-A (green) and tyrosine hydroxylase (TH, red) in the ventral mesencephali of wild-type (A–D) and Nogo-A knock-out (E–H) mouse embryos (E13.5). Dopaminergic neurons from ventral mesencephalon (A, E) are shown in higher magnification (B, F, respectively) and in single-label channels, depicting Nogo-A (C and G) or TH labeling (D and H). Arrowheads indicate TH-positive midbrain neurons, which are co-labeled with Nogo-A in the wild-type (B–D), but not in the Nogo-A knock-out ventral midbrain (F–H). Plan Apochromat 63×/1.4, zoom 3× (B–D, F–H). Scale bar = 20 μm. (For interpretation of the references to color in this figure legend, the reader is referred to the web version of this article.)

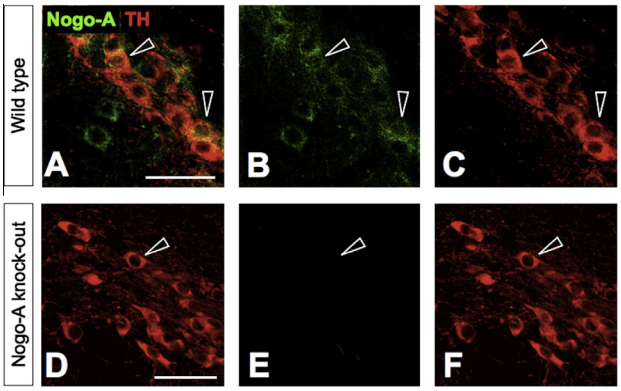

Fig. 3. Nogo-A is expressed by substantia nigra neurons of adult mice. Confocal images show double labeling of Nogo-A (green) and tyrosine hydroxylase (TH, red) in the substantiae nigrae pars compactae of adult wild-type (A–C) and Nogo-A knock-out mice (D–F). Images A and D are split into single channels depicting Nogo-A (B, E) or TH labeling (C, F) in single cells. Arrowheads indicate TH-positive nigral neurons, which are co-labeled with Nogo-A in the wild-type (A–C), but not in the Nogo-A knock-out mouse (D–F). Plan Apochromat 20×/0.8, zoom 3×/3.1×, scale bar = 50 μm. (For interpretation of the references to color in this figure legend, the reader is referred to the web version of this article.)

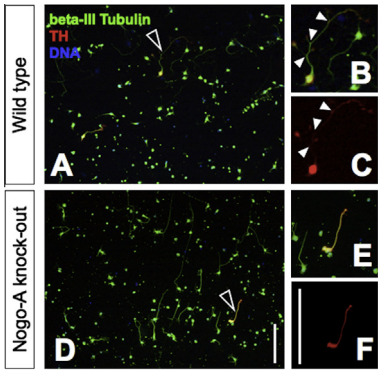

Fig. 4. Neuritic differences in dopaminergic neurons of wild-type and Nogo-A knock out mice *in vitro*. Epifluorescent images show neurons isolated from E13.5 ventral mesencephalon and labeled with tyrosine hydroxylase (TH, red), beta-III tubulin (green) and DAPI (blue, DNA binding), after 7 days *in vitro*. Differences in morphology of dopaminergic (TH-positive) neurons between wild-type (A–C) and Nogo-A knock-out mice (D–F) are exemplified. Individual neurons from wild-type and Nogo-A knock-out mice, indicated by the empty arrows (A, D, respectively) are magnified (B, E, respectively) and shown with single TH labeling (C, F, respectively). Full arrowheads (B, C) indicate the branching points present in the wild-type but absent in the Nogo-A knock-out dopaminergic neuron (E, F). Scale bar = 100 μm. (For interpretation of the references to color in this figure legend, the reader is referred to the web version of this article.)

ventral mesencephalon. Here, intense Nogo-A staining again overlapped with the intense TH immunoreactivity (Fig. 3A–C). Surrounding midbrain non-dopaminergic neurons contained lower levels or no Nogo-A. As expected, no Nogo-A labeling was present in the nigral dopaminergic neurons from the Nogo-A KO mice (Fig. 3D–F).

Our results show that Nogo-A protein is expressed by dopaminergic neurons in the mouse ventral midbrain, during development (at least 2 weeks after conception). We have also confirmed the presence of Nogo-A in mature substantia nigra pars compacta in adulthood.

Nogo-A KO, but not neutralization of cell surface Nogo-A, leads to decreased numbers of neurites and branches in ventral mesencephalon neurons *in vitro*

To investigate the role of Nogo-A in maturing dopaminergic neurons, we performed primary cultures from mouse embryonic (E13.5) ventral mesencephalon (Fig. 4). We observed differences in the morphology of neurites, in particular with regard to branching, between WT and Nogo-A KO neurons (Fig. 4B, C and E, F, respectively).

This phenomenon, as well as several other neurite growth characteristics of WT and Nogo-A KO ventral midbrain cells *in vitro,* was quantified with the aid of a Cellomics setup (Fig. 5). Additionally, to distinguish between different pools of Nogo-A (intracellular ER-bound *vs.* plasma membrane-bound), we incubated cultured dopaminergic neurons from WT mice with anti-Nogo-A specific antibody (11C7), which inhibits Nogo-A/NgR1 interactions on the cells surface. We compared the effects of Nogo-A on different parameters of neurite growth in conditions where intracellular and plasma membrane Nogo-A was active (WT), only intracellular Nogo-A was active (WT with 11C7) and where the Nogo-A was absent (Nogo-A KO). First, we assessed length, number and branching of neurites of ventral midbrain neurons labeled with antibody against beta-III tubulin, a pan-neuronal marker, which labeled 100% of our cells (data not shown). Although the average neurite length was similar in WT and Nogo-A KO neurons (about 90 μm, Fig. 5A, G, J), the number of neurites was markedly decreased when Nogo-A was absent (Fig. 5B, I, L); also the branching tended to decrease (Fig. 5C, I, L). Nogo-A-expressing neurons had on average two neurites with about three branches each per 100 μm of neurite length, whereas Nogo-A KO neurons had on average only one neurite with just one branch point per 100 μm of neurite length (Fig. 5B, C). An even stronger influence of Nogo-A on neurite length, number and branching was observed when only TH-positive/beta-III tubulin-positive (i.e. dopaminergic) neurons were analyzed (Fig. 5D–F). In contrast to Nogo-A KO condition, the neutralization of Nogo-A located on cell surface only, did not exert any inhibitory effect on neurite growth parameters, which were similar to those in the WT cells without any treatment (Fig. 5H, K).

These results suggest that Nogo-A exerts a positive role for neurite growth initiation and branching in developing mouse ventral midbrain dopaminergic and, although less pronounced, in non-dopaminergic neurons *in vitro*. This role is most likely mediated by the ER-bound Nogo-A, but not through the Nogo-A receptor complex.

Nogo-A KO does not influence the regeneration, nor the survival of nigral dopaminergic neurons upon 6-OHDA lesion in adult mice

In reference with the observations in dopaminergic cell line and primary cultures above, we explored whether the absence of Nogo-A in developing ventral

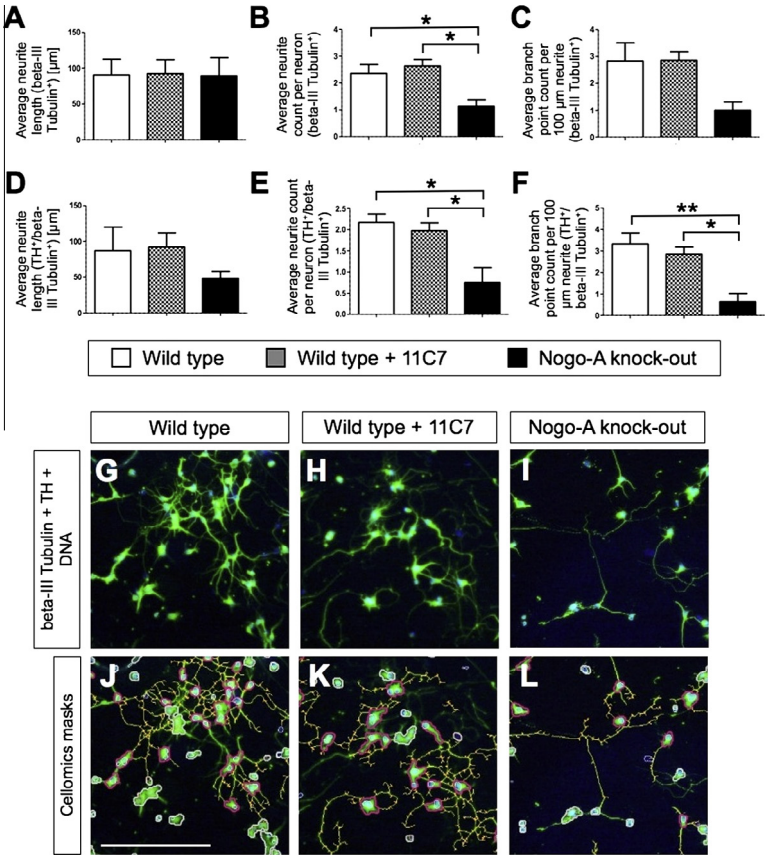

Fig. 5. Nogo-A knock-out, but not neutralizing antibody hinders neurite growth initiation and branching in dopaminergic neurons. The upper panel of the figure (A–F) depicts the Cellomics-based quantification of neurite parameters of beta-III-tubulin-positive neurons (A–C) and TH-positive/beta-III tubulin-positive (dopaminergic) neurons (D–F) from wild-type (white bars), anti-Nogo-A antibody (11C7) treated wild-type (gray bars) and Nogo-A knock-out (black bars) ventral midbrain cell cultures, obtained from E13.5 embryos. Average neurite length was similar in wild-type, 11C7-treated wild-type and Nogo-A knock-out neurons (A), likewise in dopaminergic neurons (D). The average neurite count per neuron was significantly decreased in Nogo-A knock-out cultures, when compared with the wild-type (non-treated or 11C7-treated), both in dopaminergic (E) as well as all types of neurons labeled with beta-III tubulin (B). In C, the difference in the average branch point count per 100 µm of neurite length was not statistically significant between the three groups of beta-III-tubulin-positive neurons. Though, in the case of TH-positive neurons only, Nogo-A knock-out neurons had significantly less branches per neurite fragment, than the wild-type, both in non-treated or 11C7-treated cells (F). Above parameters were assessed only for neurites longer than 25 µm, all bars represent mean of three-four independent experiments (+S.E.M.), one-way ANOVA and Tukey's post hoc test, A ($F(2,12) = 0.003$, $p = 0.996$), B ($F(2,12) = 7.872$, $p = 0.016$), C ($F(2,12) = 4.83$, $p = 0.042$), D ($F(2,12) = 1.09$, $p = 0.395$), E ($F(2,12) = 7.546$, $p = 0.0144$), F ($F(2,12) = 13.15$, $p = 0.0043$). The lower panel (G–L) shows the examples of the images employed in Cellomics analysis (G–H, same immuno-labeling as in Fig. 4) and the images of masks generated by the software (J–L) in three different conditions (wild-type – G, J, Wild-type and 11C7 – H, K Nogo-A knock-out – I, L). In J, K the included cell nuclei (pink), excluded cell nuclei (white), neurites (yellow) and 'neurite points' (yellow dots) are marked. Scale bar = 100 µm. (For interpretation of the references to color in this figure legend, the reader is referred to the web version of this article.)

mesencephalic dopaminergic neurons would have any impact on the dopaminergic nigrostriatal network formation and neuronal survival in the adult mice.

First, we compared the striatal dimensions as well as optical intensity of the TH-stained fibers (striatal axonal network, formed by the TH-positive fibers originating from the substantia nigra neurons) in their main target, the neostriatum (Fig. 6A, B) in intact WT and Nogo-A KO mice (Fig. 6E). We did not observe any differences between WT and Nogo-A KO mice (Fig. 6E and data not shown). We then analyzed axonal arbors and dopaminergic cell survival upon lesion with the neurotoxin 6-OHDA (specifically toxic for dopaminergic neurons). 6-OHDA was injected into the right striatum. Four days after the lesion, the optical intensity of TH-positive fibers in the neostriatum was reduced to 29 ± 7% (average ± S.E.M.) in the WT and 43 ± 5% in the Nogo-A KO mice (Fig. 6F) comparing to the intact striatum. Four weeks after the lesion, both WT and KO mice showed a reduction to about 50% of TH-positive axons in the striatum (48 ± 6% and 46 ± 1% remaining fibers, respectively; Fig. 6F). Eight weeks after the 6-OHDA injection, the dopaminergic striatal innervation was reduced to 69 ± 4% in the WT mice and to 79 ± 5% in the Nogo-A KO mice (Fig. 6F). The differences between WT and KO mice were not statistically significant at any time point. Furthermore, we compared optical densities of TH immunostaining separately in the four quadrants of the striatum: dorso-medial, medio-lateral, ventro-lateral and ventro-medial, which reflect different nigrostriatal projections. Again, we did not observe statistically significant differences in TH-fiber denervation at any time point between WT and Nogo-A KO animals (data not shown).

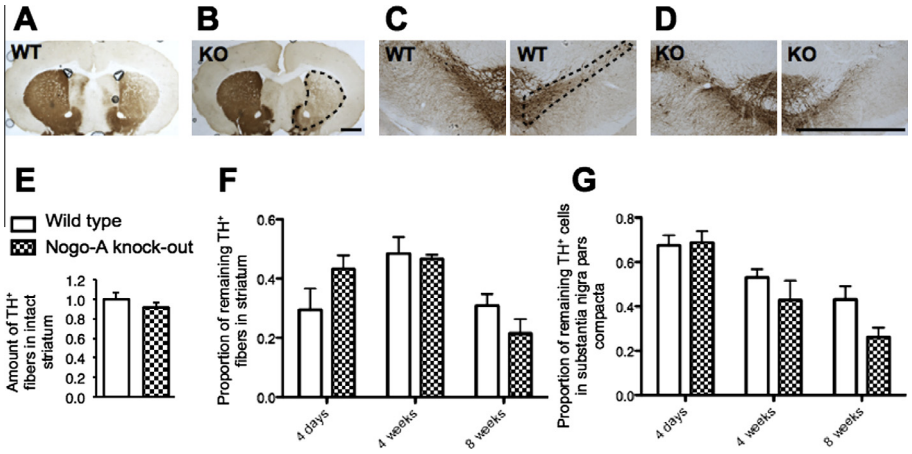

Fig. 6. Dopaminergic fiber and cell degeneration in wild-type and Nogo-A knock-out mice after 6-OHDA lesion. Four days, 4 weeks and 8 weeks after unilateral striatal 6-OHDA lesion, brain sections from wild-type ('WT', A, C) and Nogo-A knock-out mice ('KO', B, D) were stained with tyrosine hydroxylase (TH). The images exemplify the degree of dopaminergic fiber (A, B) and dopaminergic cell loss (C, D) 8 weeks after the lesion (in the right hemisphere). TH-positive fiber amounts (assessed by densitometry, E, F) and TH-positive neuron loss (assessed by neuron counts, G) were quantified in areas marked by dashed lines (B, C, respectively), in only intact (E) or both hemispheres (F, G). In E, the values from KO were expressed referring to WT ('4 weeks' time point); in both F and G, the value obtained by the same kind of measurement on the non-lesioned side of the section served as a reference. The bars represent the average with S.E.M., $n = 5–10$, in F and G: two-way ANOVA (F – time $F(1,42) = 7.55$, $p = 0.0016$; genotype $F(1,42) = 0.040$, $p = 0.843$; interaction $F(1,42) = 2.516$, $p = 0.093$; G – time $F(1,43) = 22.77$, $p < 0.0001$; genotype $F(1,43) = 4.08$, $p = 0.0497$; interaction $F(2,43) = 1.70$, $p = 0.195$); Scale bar = 1000 μm.

Finally, we assessed cell death in substantia nigra pars compacta by quantifying the remaining TH-positive cells in left and right midbrain 4 days, 4 weeks or 8 weeks after the unilateral striatal 6-OHDA injection (Fig. 6C, D, G). The proportion of remaining cells diminished gradually from 4 days to 8 weeks after the lesions (Fig. 6G). Four days and 4 weeks after the lesion, the cell loss in substantia nigra was comparable between WT and Nogo-A KO mice: on average 69% cells remained after 4 days while about 50% remained after 4 weeks (Fig. 6G). Interestingly, 8 weeks after the lesion a statistically non-significant trend toward more pronounced cell death of dopaminergic cells was evident in the substantia nigra of Nogo-A KO mice (26 ± 4% surviving neurons) compared to the WT mice (45 ± 6% surviving cells; Fig. 6G). These results suggest that in adult nigral dopaminergic neurons, Nogo-A might contribute to resistance against toxic insults. Though, such hypothesis requires further investigation.

DISCUSSION

We show that Nogo-A protein is present in the cytoplasm of the developing ventral mesencephalic neurons in human cell line and mice. In immature dopaminergic neurons *in vitro*, intracellular Nogo-A has a positive influence on the initiation and branching of neurites.

Midbrain dopaminergic neurons express Nogo-A during development

Nogo-A has previously been shown to be present in dopaminergic substantia nigra neurons of adult mice (Wang et al., 2002). Colorimetric labeling in neuromelanin-enriched nigral neurons did not definitively confirm the presence of Nogo-A in this region in human (Buss et al., 2005). Here we found that a ventral mesencephalon-derived human cell line expresses Nogo-A, and that the protein is upregulated during dopaminergic differentiation of these cells. We have also detected Nogo-A in ventral mesencephalic dopaminergic neurons of mice, both in the embryonic (E13.5) and adult brains. It is evident that the majority of Nogo-A in midbrain dopaminergic neurons is intracellular.

Intracellular Nogo-A facilitates initiation and branching of neurites in midbrain neurons

Upon differentiation and neurite outgrowth, protein levels of Nogo-A increase (about threefold) in the human mesencephalic cell line. This observation is in line with previous reports where the enrichment of Nogo-A expression in different types of maturing neurons with growing neurites has been shown. Growing axons of the olfactory tract expressed Nogo-A *in vivo* (Tozaki et al., 2002) and *in vitro.* Nogo-A accumulated at axonal branch points and the central domain of the growth cones, co-expressed with growth-associated proteins (Richard et al., 2005). Similarly, Nogo-A was enriched in the axonal varicosities and growth cones in embryonic cortical neurons *in vitro* (Hunt et al., 2003). From those morphological studies, Nogo-A's positive role in axonal extension could be anticipated.

Nevertheless, the functional studies where neuronal Nogo-A was deleted or its activity was neutralized with specific antibodies showed that both, growth promoting and inhibitory effects of Nogo-A exist in growing neurites and migrating neurons, depending on neuronal type and probably also developmental stage.

For instance, Nogo-A/B/C KO hampered the tangential migration of interneurons into the embryonic

cortex, and the cortical neurons *in vitro* showed earlier polarization and increased branching vs. the WT condition (Mingorance-Le Meur et al., 2007). In contrast, an enhanced radial migration of the cortical neurons along the radial glial fibers was reported upon treatments with anti-Nogo-A antibodies or KO, both *in vivo* and *in vitro* (Mathis et al., 2010). Interestingly, in the cerebellar Purkinje cells genetically depleted from Nogo-A, the dendritic trees were larger and more complex, comparing to WT or Nogo-A overexpressing Purkinje cells (Petrinovic et al., 2013) suggesting Nogo-A's negative role in neurite growth in this cell type. Contrastingly, in regenerating retinal ganglion cells *in vivo*, Nogo-A overexpression in the neurons enhanced, whereas Nogo-A inhibition diminished regenerative sprouting (Pernet et al., 2012). Similarly, decreased branching, increased neurite fasciculation and longer neurites were observed upon Nogo-A signaling depletion in dorsal root ganglion cell cultures (Petrinovic et al., 2010).

In our study, we observed that midbrain neurons lacking Nogo-A had fewer processes and fewer branches, when compared to their WT counterparts. Such an effect was not observed when only intracellular Nogo-A was active. This suggests that Nogo-A has perhaps a neurite-growth-promoting role in neurons of ventral midbrain *in vitro* and it is probably not mediated via Nogo-A receptor complex but rather via ER-localized Nogo-A.

In the adult mice, the density of TH labeling in the striatum seem not to be affected by the Nogo-A KO. This may be attributed to compensatory mechanisms, which occur frequently in different models of gene KO. Indeed, increased levels of certain semaphorins and ephrins and their receptors have been seen in the CNS of mice lacking Nogo-A (Kempf et al., 2013) and also Nogo-B was shown to be up-regulated in Nogo-A KO mice (Simonen et al., 2003; Dimou et al., 2006).

CONCLUSION

Although Nogo-A is mostly expressed in oligodendrocytes and myelin in the adult CNS, neuronal expression is prevalent during development and includes midbrain dopaminergic neurons. We show that Nogo-A facilitates neurite formation and branching of neurites in the developing midbrain dopaminergic and non-dopaminergic neurons, and this function is attributed to the intracellular ER-bound Nogo-A. These results make Nogo-A an interesting target for further studies in particular in the context of Parkinson's disease.

Acknowledgments—We would like to thank Birgit Haraldsson and Dr. Xiaoyi Zou for excellent technical support in in vivo experiments. We would like to thank Dr. Marcel Leist for providing us the LUHMES cells in the project. The study is supported by grants from the Swedish Research Council, and by the Marie Curie Initial Training Network "Axonal regeneration, plasticity & stem cells" (AXREGEN). We would like to acknowledge Andy McCourt for the critical reading and linguistic revision of the manuscript.

REFERENCES

Bandtlow CE, Dlaska M, Pirker S, Czech T, Baumgartner C, Sperk G (2004) Increased expression of Nogo-A in hippocampal neurons of patients with temporal lobe epilepsy. Eur J Neurosci 20:195–206.

Bossers K, Meerhoff G, Balesar R, van Dongen JW, Kruse CG, Swaab DF, Verhaagen J (2009) Analysis of gene expression in Parkinson's disease: possible involvement of neurotrophic support and axon guidance in dopaminergic cell death. Brain Pathol 19:91–107.

Buss A, Sellhaus B, Wolmsley A, Noth J, Schwab ME, Brook GA (2005) Expression pattern of NOGO-A protein in the human nervous system. Acta Neuropathol 110:113–119.

Caroni P, Schwab ME (1988) Antibody against myelin-associated inhibitor of neurite growth neutralizes nonpermissive substrate properties of CNS white matter. Neuron 1:85–96.

Chen MS, Huber AB, van der Haar ME, Frank M, Schnell L, Spillmann AA, Christ F, Schwab ME (2000) Nogo-A is a myelin-associated neurite outgrowth inhibitor and an antigen for monoclonal antibody IN-1. Nature 403:434–439.

Choi HK, Won L, Roback JD, Wainer BH, Heller A (1992) Specific modulation of dopamine expression in neuronal hybrid cells by primary cells from different brain regions. Proc Natl Acad Sci U S A 89:8943–8947.

Choi HK, Won LA, Kontur PJ, Hammond DN, Fox AP, Wainer BH, Hoffmann PC, Heller A (1991) Immortalization of embryonic mesencephalic dopaminergic neurons by somatic cell fusion. Brain Res 552:67–76.

Chu Y, Kompoliti K, Cochran EJ, Mufson EJ, Kordower JH (2002) Age-related decreases in Nurr1 immunoreactivity in the human substantia nigra. J Comp Neurol 450:203–214.

Delekate A, Zagrebelsky M, Kramer S, Schwab ME, Korte M (2011) NogoA restricts synaptic plasticity in the adult hippocampus on a fast time scale. Proc Natl Acad Sci U S A 108:2569–2574.

Dimou L, Schnell L, Montani L, Duncan C, Simonen M, Schneider R, Liebscher T, Gullo M, Schwab ME (2006) Nogo-A-deficient mice reveal strain-dependent differences in axonal regeneration. J Neurosci 26:5591–5603.

Dodd DA, Niederoest B, Bloechlinger S, Dupuis L, Loeffler JP, Schwab ME (2005) Nogo-A, -B, and -C are found on the cell surface and interact together in many different cell types. J Biol Chem 280:12494–12502.

Emborg ME, Ma SY, Mufson EJ, Levey AI, Taylor MD, Brown WD, Holden JE, Kordower JH (1998) Age-related declines in nigral neuronal function correlate with motor impairments in rhesus monkeys. J Comp Neurol 401:253–265.

Fournier AE, Takizawa BT, Strittmatter SM (2003) Rho kinase inhibition enhances axonal regeneration in the injured CNS. J Neurosci 23:1416–1423.

Hamza TH, Zabetian CP, Tenesa A, Laederach A, Montimurro J, Yearout D, Kay DM, Doheny KF, Paschall J, Pugh E, Kusel VI, Collura R, Roberts J, Griffith A, Samii A, Scott WK, Nutt J, Factor SA, Payami H (2010) Common genetic variation in the HLA region is associated with late-onset sporadic Parkinson's disease. Nature genetics 42:781–785.

Hornykiewicz O (1966) Dopamine (3-hydroxytyramine) and brain function. Pharmacol Rev 18:925–964.

Huber AB, Weinmann O, Brosamle C, Oertle T, Schwab ME (2002) Patterns of Nogo mRNA and protein expression in the developing and adult rat and after CNS lesions. J Neurosci 22:3553–3567.

Hunt D, Coffin RS, Prinjha RK, Campbell G, Anderson PN (2003) Nogo-A expression in the intact and injured nervous system. Mol Cell Neurosci 24:1083–1102.

Ivanova T, Beyer C (2003) Estrogen regulates tyrosine hydroxylase expression in the neonate mouse midbrain. J Neurobiol 54:638–647.

Kapfhammer JP, Schwab ME (1994) Inverse patterns of myelination and GAP-43 expression in the adult CNS: neurite growth inhibitors as regulators of neuronal plasticity? J Comp Neurol 340:194–206.

Kempf A, Montani L, Petrinovic MM, Schroeter A, Weinmann O, Patrignani A, Schwab ME (2013) Upregulation of axon guidance molecules in the adult CNS of Nogo-A KO mice restricts neuronal growth and regeneration. Eur J Neurosci, in press. [Epub ahead of print].

Lackner P, Beer R, Broessner G, Helbok R, Dallago K, Hess MW, Pfaller K, Bandtlow C, Schmutzhard E (2011) Nogo-A expression in the brain of mice with cerebral malaria. PLoS One 6:e25728.

Lesnick TG, Papapetropoulos S, Mash DC, Ffrench-Mullen J, Shehadeh L, de Andrade M, Henley JR, Rocca WA, Ahlskog JE, Maraganore DM (2007) A genomic pathway approach to a complex disease: axon guidance and Parkinson disease. PLoS Genet 3:e98.

Lotharius J, Barg S, Wiekop P, Lundberg C, Raymon HK, Brundin P (2002) Effect of mutant alpha-synuclein on dopamine homeostasis in a new human mesencephalic cell line. J Biol Chem 277:38884–38894.

Lotharius J, Falsig J, van Beek J, Payne S, Dringen R, Brundin P, Leist M (2005) Progressive degeneration of human mesencephalic neuron-derived cells triggered by dopamine-dependent oxidative stress is dependent on the mixed-lineage kinase pathway. J Neurosci 25:6329–6342.

Mathis C, Schroter A, Thallmair M, Schwab ME (2010) Nogo-a regulates neural precursor migration in the embryonic mouse cortex. Cereb Cortex 20:2380–2390.

Maxwell SL, Ho HY, Kuehner E, Zhao S, Li M (2005) Pitx3 regulates tyrosine hydroxylase expression in the substantia nigra and identifies a subgroup of mesencephalic dopaminergic progenitor neurons during mouse development. Dev Biol 282:467–479.

McGee AW, Yang Y, Fischer QS, Daw NW, Strittmatter SM (2005) Experience-driven plasticity of visual cortex limited by myelin and Nogo receptor. Science 309:2222–2226.

Mingorance-Le Meur A, Zheng B, Soriano E, del Rio JA (2007) Involvement of the myelin-associated inhibitor Nogo-A in early cortical development and neuronal maturation. Cereb Cortex 17:2375–2386.

Montani L, Gerrits B, Gehrig P, Kempf A, Dimou L, Wollscheid B, Schwab ME (2009) Neuronal Nogo-A modulates growth cone motility via Rho-GTP/LIMK1/cofilin in the unlesioned adult nervous system. J Biol Chem 284:10793–10807.

Oertle T, van der Haar ME, Bandtlow CE, Robeva A, Burfeind P, Buss A, Huber AB, Simonen M, Schnell L, Brosamle C, Kaupmann K, Vallon R, Schwab ME (2003) Nogo-A inhibits neurite outgrowth and cell spreading with three discrete regions. J Neurosci 23:5393–5406.

Pernet V, Joly S, Dalkara D, Schwarz O, Christ F, Schaffer D, Flannery JG, Schwab ME (2012) Neuronal Nogo-A upregulation does not contribute to ER stress-associated apoptosis but participates in the regenerative response in the axotomized adult retina. Cell Death Differ 19:1096–1108.

Petrinovic MM, Duncan CS, Bourikas D, Weinman O, Montani L, Schroeter A, Maerki D, Sommer L, Stoeckli ET, Schwab ME (2010) Neuronal Nogo-A regulates neurite fasciculation, branching and extension in the developing nervous system. Development 137:2539–2550.

Petrinovic MM, Hourez R, Aloy EM, Dewarrat G, Gall D, Weinmann O, Gaudias J, Bachmann LC, Schiffmann SN, Vogt KE, Schwab ME (2013) Neuronal Nogo-A negatively regulates dendritic morphology and synaptic transmission in the cerebellum. Proc Natl Acad Sci U S A 110:1083–1088.

Pruszak J, Just L, Isacson O, Nikkhah G (2009) Isolation and culture of ventral mesencephalic precursor cells and dopaminergic neurons from rodent brains. Curr Protoc Stem Cell Biol [Chapter 2:Unit 2D 5], Wiley Online Library.

Raiker SJ, Lee H, Baldwin KT, Duan Y, Shrager P, Giger RJ (2010) Oligodendrocyte-myelin glycoprotein and Nogo negatively regulate activity-dependent synaptic plasticity. J Neurosci 30:12432–12445.

Richard M, Giannetti N, Saucier D, Sacquet J, Jourdan F, Pellier-Monnin V (2005) Neuronal expression of Nogo-A mRNA and protein during neurite outgrowth in the developing rat olfactory system. Eur J Neurosci 22:2145–2158.

Rick CE, Ebert A, Virag T, Bohn MC, Surmeier DJ (2006) Differentiated dopaminergic MN9D cells only partially recapitulate the electrophysiological properties of midbrain dopaminergic neurons. Dev Neurosci 28:528–537.

Riederer P, Wuketich S (1976) Time course of nigrostriatal degeneration in parkinson's disease. A detailed study of influential factors in human brain amine analysis. J Neural Transm 38:277–301.

Schildknecht S, Poltl D, Nagel DM, Matt F, Scholz D, Lotharius J, Schmieg N, Salvo-Vargas A, Leist M (2009) Requirement of a dopaminergic neuronal phenotype for toxicity of low concentrations of 1-methyl-4-phenylpyridinium to human cells. Toxicol Appl Pharmacol 241:23–35.

Scholz D, Poltl D, Genewsky A, Weng M, Waldmann T, Schildknecht S, Leist M (2011) Rapid, complete and large-scale generation of post-mitotic neurons from the human LUHMES cell line. J Neurochem 119:957–971.

Schwab ME (2010) Functions of Nogo proteins and their receptors in the nervous system. Nat Rev Neurosci 11:799–811.

Simonen M, Pedersen V, Weinmann O, Schnell L, Buss A, Ledermann B, Christ F, Sansig G, van der Putten H, Schwab ME (2003) Systemic deletion of the myelin-associated outgrowth inhibitor Nogo-A improves regenerative and plastic responses after spinal cord injury. Neuron 38:201–211.

Tews B, Schonig K, Arzt ME, Clementi S, Rioult-Pedotti MS, Zemmar A, Berger SM, Schneider M, Enkel T, Weinmann O, Kasper H, Schwab ME, Bartsch D (2013) Synthetic microRNA-mediated downregulation of Nogo-A in transgenic rats reveals its role as regulator of synaptic plasticity and cognitive function. Proc Natl Acad Sci U S A 110:6583–6588.

Tozaki H, Kawasaki T, Takagi Y, Hirata T (2002) Expression of Nogo protein by growing axons in the developing nervous system. Brain Res Mol Brain Res 104:111–119.

Wang X, Chun SJ, Treloar H, Vartanian T, Greer CA, Strittmatter SM (2002) Localization of Nogo-A and Nogo-66 receptor proteins at sites of axon-myelin and synaptic contact. J Neurosci 22:5505–5515.

Yiu G, He Z (2006) Glial inhibition of CNS axon regeneration. Nat Rev Neurosci 7:617–627.

Zagrebelsky M, Schweigreiter R, Bandtlow CE, Schwab ME, Korte M (2010) Nogo-A stabilizes the architecture of hippocampal neurons. J Neurosci 30:13220–13234.

Zhou QY, Quaife CJ, Palmiter RD (1995) Targeted disruption of the tyrosine hydroxylase gene reveals that catecholamines are required for mouse fetal development. Nature 374:640–643.

(Accepted 13 October 2013)
(Available online 21 October 2013)